Acta Crystallographica Section F
Structural Biology and Crystallization Communications
ISSN 1744-3091

Structure of the catalytic trimer of *Methanococcus jannaschii* aspartate transcarbamoylase in an orthorhombic crystal form

Jacqueline Vitali[a]* and Michael J. Colaneri[b]

[a]Department of Physics, Cleveland State University, Euclid Avenue at East 24th Street, Cleveland, OH 44115, USA, and [b]Department of Chemistry and Physics, SUNY College at Old Westbury, Old Westbury, NY 11568, USA

Correspondence e-mail: j.vitali@csuohio.edu

Received 15 May 2008
Accepted 6 August 2008

PDB Reference: aspartate transcarbamoylase, 3e2p, r3e2psf.

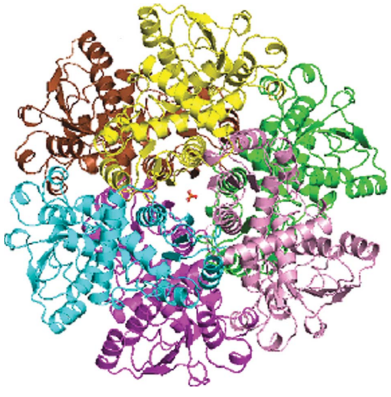

Crystals of the catalytic subunit of *Methanococcus jannaschii* aspartate transcarbamoylase in an orthorhombic crystal form contain four crystallographically independent trimers which associate in pairs to form stable staggered complexes that are similar to each other and to a previously determined monoclinic *C*2 form. Each subunit has a sulfate in the central channel. The catalytic subunits in these complexes show flexibility, with the elbow angles of the monomers differing by up to 7.4° between crystal forms. Moreover, there is also flexibility in the relative orientation of the trimers around their threefold axis in the complexes, with a difference of 4° between crystal forms.

1. Introduction

Aspartate transcarbamoylase (ATCase; EC 2.1.3.2) catalyzes the second step of *de novo* pyrimidine biosynthesis, the reaction between carbamoyl phosphate (CP) and aspartate to form *N*-carbamoyl-L-aspartate and inorganic phosphate (Jones *et al.*, 1955), and is an important site of regulation of this pathway in many organisms. The structure and properties of the *Escherichia coli* enzyme have been extensively studied (Herve, 1989; Allewell, 1989; Lipscomb, 1992, 1994; England *et al.*, 1994). It has a dodecameric structure (C_6R_6) composed of two types of subunits. The two larger or catalytic subunits (C_3) are each composed of three identical polypeptide chains (M_r 33 000), while the three smaller or regulatory subunits (R_2) are each composed of two identical polypeptide chains (M_r 17 000). The catalytic chains contain two domains: the carbamoyl phosphate (CP) and aspartate-binding (ASP) domains. The regulatory chains also contain two domains: the nucleotide and Zn-binding domains. *E. coli* ATCase is an allosteric enzyme that exhibits cooperativity for aspartate and heterotropic effects, being activated by ATP and inhibited by CTP. Upon binding the substrate aspartate (in the presence of saturating CP), *E. coli* ATCase undergoes a conformational change from a low-activity T state to a higher activity R state. The large conformational differences in the X-ray structures of the unliganded ATCase (Stevens *et al.*, 1990*a*,*b*) and the *N*-phosphonacetyl-L-aspartate (PALA) liganded enzyme (Ke *et al.*, 1988; Jin *et al.*, 1999) have been proposed to define the structural differences between the T and R states.

Characterization of the ATCase enzyme from the hyperthermophilic and barophilic archaeon *Methanococcus jannaschii* (Hack *et al.*, 2000) suggested that it consists of catalytic trimers and regulatory dimers and has a molecular weight similar to that from *E. coli*. Kinetic analysis of *M. jannaschii* ATCase from cell-free extracts showed that it has limited homotropic cooperativity and little if any regulatory properties with ATP and CTP. Kinetic analysis of the *M. jannaschii* catalytic trimer showed hyperbolic kinetics with an activation energy similar to that of the *E. coli* trimer and with an activity that increases with temperature. It is stable at 358 K.

We have previously determined the structure of the catalytic trimer of *M. jannaschii* ATCase in a monoclinic crystal form (Vitali *et al.*, 2008). This study and comparisons with *E. coli* ATCase and the

Table 1
Data-collection and final refinement statistics.

Values in parentheses are for the highest resolution shell.

Summary of X-ray diffraction data collection	
Space group	$P2_12_12_1$
Unit-cell parameters (Å)	a = 87.13, b = 167.93, c = 319.41
Resolution range (Å)	40.0–3.0 (3.1–3.0)
Temperature (K)	100
Wavelength (Å)	0.979
No. of unique reflections	92280
Redundancy	4.4 (2.8)
Completeness (%)	99.5 (96.8)
Mean $I/\sigma(I)$	8.9 (1.4)
$R_{\rm merge}$†	0.095 (0.67)
Final refinement statistics	
Resolution range (Å)	40.0–3.0
No. of reflections	86463‡
Non-H protein atoms per ASU	29609
Waters per ASU	500
Sulfates per ASU	4
$R_{\rm work}$§	0.215
$R_{\rm free}$§	0.269
R.m.s. deviations from ideal geometry	
Bond lengths (Å)	0.01
Bond angles (°)	1.3
Impropers (°)	0.8
B values (Å^2)	
From Wilson plot	73.3
Mean B over all atoms	70.0
Ramachandran plot	
Most favored regions (%)	84.5
Additional allowed regions (%)	13.9
Generously allowed regions (%)	1.1
Disallowed regions (%)	0.5¶

† $R_{\rm merge} = \sum_{hkl}\sum_i |I_i(hkl) - \langle I(hkl)\rangle| / \sum_{hkl}\sum_i I_i(hkl)$, where $I_i(hkl)$ and $\langle I(hkl)\rangle$ are the observed intensity of measurement i and the mean intensity of the reflection with indices hkl, respectively. ‡ The number of reflections used in the refinement differs from the number scaled because reflections with $|F_o(hkl)| = 0$ were excluded. § $R_{\rm work}$ and $R_{\rm free} = \sum_{hkl} \big||F_o(hkl)| - |F_c(hkl)|\big| / \sum_{hkl} |F_o(hkl)|$, where $|F_o(hkl)|$ and $|F_c(hkl)|$ are the observed and calculated structure-factor amplitudes, respectively. $R_{\rm work}$ is calculated for the reflections used in the refinement (90% of data) and $R_{\rm free}$ for the reflections used in the test set (10% of data). ¶ Except for Leu263, all residues in this region, namely Ser128 of C6 (complex 1) and C1 (complex 2), Asn129 of C1 (complex 1), C5 (complex 1), C1 (complex 2) and C4 (complex 2) and Glu82 of C4 (complex 1), correspond to poor electron density.

hyperthermophilic ATCases from *Pyrococcus abyssi* (Van Boxstael *et al.*, 2003) and *Sulfolobus acidocaldarius* (De Vos *et al.*, 2004) provided insight into the strategies for thermostabilization adopted by the *M. jannaschii* enzyme. We undertook the structural analysis of the orthorhombic form which is presented in this paper in order to further investigate the structure of the enzyme in different crystalline environments and its thermostabilization strategies. In particular, we were interested in the possible patterns of association of the catalytic subunits in the crystal. An interesting feature of the monoclinic form was the vertical association of two crystallographically independent catalytic subunits into a staggered dimer of trimers.

2. Materials and methods

2.1. Protein preparation and crystallization

The *M. jannaschii* catalytic trimer was prepared following the procedure of Hack *et al.* (2000) from *E. coli* strain EK1911 which has a deletion in the *pyrBI* region of the chromosome and contains the plasmids pEK406 coding for the *M. jannaschii* catalytic chain and pSJS1240 (Kim *et al.*, 1998) coding for rare archaeal tRNAs. The gene for the *M. jannaschii* catalytic chain is not associated with any tags in pEK406. The purification involved a 30% ammonium sulfate precipitation step, a heat step at 363 K for 15 min and chromatography using a Q-Sepharose Fast Flow anion-exchange column and a phenyl Sepharose column. The purified protein was concentrated to 15 mg ml^{-1} in 40 m*M* KH_2PO_4, 0.2 m*M* EDTA and 2 m*M* 2-mercaptoethanol pH 7.0. Crystals were grown at 295 K by the sitting-drop method from reservoirs containing 2.5 *M* ammonium sulfate and 0.1 *M* Tris–HCl pH 8.5. The drops consisted of 5 µl reservoir solution and 5 µl protein solution. Two crystals were used for this study: they belonged to space group $P2_12_12_1$, with unit-cell parameters (average for the two crystals) a = 87.13, b = 167.93, c = 319.41 Å, four trimers per asymmetric unit and a $V_{\rm M}$ of 2.80 Å^3 Da^{-1} (Matthews, 1968).

2.2. X-ray data collection

Diffraction data were measured on the X12B beamline of the National Synchrotron Light Source at Brookhaven National Laboratory using an ADSC Quantum-4 CCD detector. The temperature was 100 K, the wavelength was 0.979 Å and the crystal-to-detector distance was 340.00 mm. The cryoprotectant used was 15% glucose. Two crystals were used. Oscillations were measured for 60 s each in 1.0° intervals of φ. A range of 100° in φ was measured for the first crystal and a range of 70° for the second. The data were processed with the *HKL* software package (Otwinowski & Minor, 1997). The data from the two crystals were reduced and integrated in *DENZO* and merged and scaled in *SCALEPACK*. Data statistics are summarized in Table 1.

2.3. Structure determination and refinement

The structure was solved using molecular replacement by evolutionary search with *EPMR* (Kissinger *et al.*, 1999) and data in the 15.0–4.0 Å resolution range. The search model was the complex of the two trimers in the asymmetric unit of the monoclinic form (Vitali *et al.*, 2008). Refinement was carried out with *CNS* (Brünger *et al.*, 1998) using simulated annealing with torsion-angle dynamics. During the refinement NCS restraints were imposed for both the main chain and side chains for most of the four regions 1–131, 132–146, 147–280 and 281–303 among the 12 monomers. Residues that appeared to differ between monomers were refined independently. The refinement was alternated with manual model building and rebuilding using *O* (Jones *et al.*, 1991) and *Coot* (Emsley & Cowtan, 2004). Model building was facilitated by electron-density maps computed with phases improved by solvent flipping, density truncation and NCS averaging over all 12 monomers. For each amino acid, two group temperature factors were refined: one for the main chain and one for the side chain. Each trimer had a sulfate in its central tunnel on the noncrystallographic threefold. The sulfates were harmonically restrained to their initial positions as well as with respect to each other together with residues 55–67 of the monomers in each trimer. At the end of the analysis, waters were added to the model using as criteria a 2σ peak height in the difference maps and hydrogen-bonding distances to protein atoms of 2.0–3.5 Å.

2.4. Model analysis

The quality of the structure was analyzed with *PROCHECK* (Laskowski *et al.*, 1993). Hydrogen bonds were calculated with *HBPLUS* (McDonald & Thornton, 1994) using donor–acceptor distances of less that 3.5 Å, hydrogen–acceptor distances of less than 2.5 Å and associated angles greater than 90°. Salt bridges between two charged groups corresponded to distances of less than 4.0 Å. A hydrophobic contact was assumed to exist between two apolar residues if the carbon–carbon distance was less than 4.0 Å. *DSSP* (Kabsch & Sander, 1983) was used for computing accessible surface areas (ASAs). Structure superpositions were performed with

LSQMAN (Kleywegt, 1996). Figures were prepared with *PyMOL* (http://pymol.sourceforge.net).

The planar angles between the CP and ASP domains were computed by a modification of the method of Williams *et al.* (1998) using the angle between the geometric centers of the two domains and a hinge point. The geometric centers for the CP and ASP domains in *M. jannaschii* were computed from the C^{α} atoms of residues 1–131 and 147–280, respectively. The hinge point was taken as the C^{α} atom of residue 137. The corresponding residues were used in the computation of the angles in the other ATCases.

The global association of two catalytic subunits in a complex is described by the distance between their geometric centers and the torsion angle between the individual chains of the two subunits around the axis defined by this line. The geometric centers were computed from the C^{α} atoms of residues 1–131 and 147–280.

2.5. Dynamic light-scattering measurements

Dynamic light-scattering measurements were carried out by the W. M. Keck Foundation Biotechnology Laboratory, Yale University, New Haven, Connecticut at 0.66 *M* ammonium sulfate and a protein concentration of 5.0 mg ml^{-1} using a DynaPro 99-362.

3. Results and discussion

3.1. Quality of the structure

The final model consists of two crystallographically independent complexes consisting of trimers, four sulfates and 500 waters. Final refinement statistics are presented in Table 1. All the stereochemical parameters are within the range expected for a model at this resolution. In the Ramachandran plot computed in *PROCHECK* (Laskowski *et al.*, 1993), 84.5% of the residues are found in the most favorable regions. Leu263 is in a disallowed region, as is often the case for active-site residues. This residue is also found in disallowed regions in the PALA-liganded and unliganded *E. coli* catalytic subunit (Endrizzi *et al.*, 2000; Beernink *et al.*, 1999) and holoenzyme (Jin *et al.*, 1999; Stevens *et al.*, 1990*a*,*b*) and in the PALA-liganded *P. abyssi* catalytic trimer (Van Boxstael *et al.*, 2003). The two complexes have different average temperature factors (complex 1, 54.1 $Å^2$; complex 2, 86.6 $Å^2$), probably because they form different

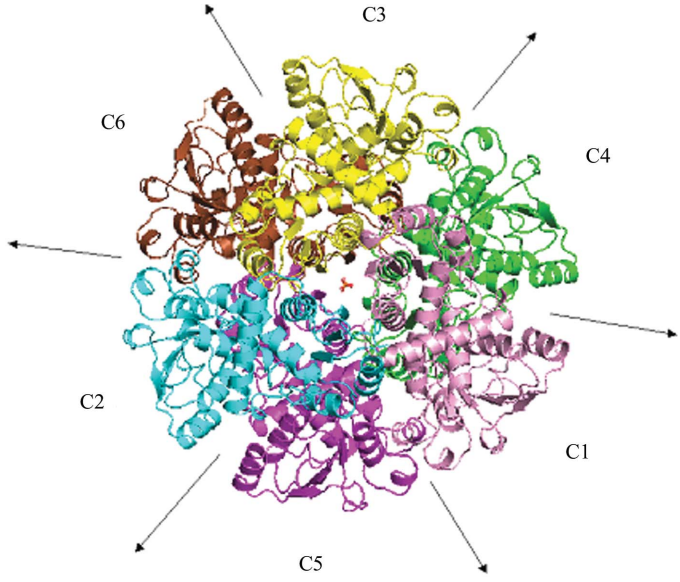

(*a*)

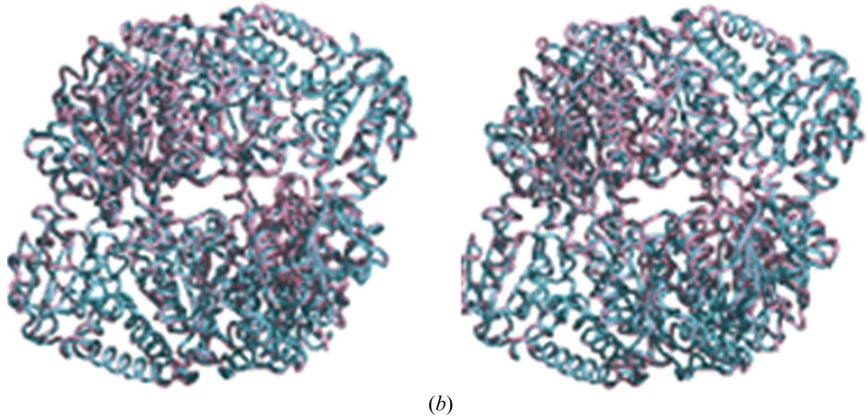

(*b*)

Figure 1
(*a*) View of one of the *M. jannaschii* complexes in the asymmetric unit (complex 1) looking down the noncrystallographic threefold. Each monomer is depicted in a different color. Both sulfates on the noncrystallographic threefold are shown. Arrows denote the noncrystallographic twofold axes. The catalytic chains C1, C2 and C3 comprise the top trimer of the complex, while the C4, C5 and C6 chains comprise the bottom subunit. (*b*) Side stereoview of the two *M. jannaschii* complexes in the present structure superimposed on each other. Complex 1 is shown in pink and complex 2 is shown in teal. The view is looking down the noncrystallographic twofold.

Table 2
Comparison of the planar angles of the *M. jannaschii* catalytic trimer in the orthorhombic form with the monoclinic form and other systems.

PDB codes used were *M. jannaschii* monoclinic form, 2rgw (Vitali *et al.*, 2008); *E. coli* catalytic trimer, 3csu (Beernink *et al.*, 1999); *P. abyssi* catalytic trimer + PALA, 1ml4 (Van Boxstael *et al.*, 2003); *E. coli* catalytic trimer + PALA, 1ekx (Endrizzi *et al.*, 2000); *S. acidocaldarius* T-form ATCase, 1pg5 (De Vos *et al.*, 2004); *E. coli* T-form ATCase, 6at1 (Stevens *et al.*, 1990*a*,*b*); *E. coli* R-form ATCase, 1d09 (Jin *et al.*, 1999). Values for crystallographically independent chains are separated by commas.

System	Planar angles (°)
M. jannaschii orthorhombic form	
Complex 1, C1C2C3	124.7, 124.3, 123.8
Complex 1, C4C5C6	124.3, 122.9, 124.1
Complex 2, C1C2C3	124.7, 125.2, 124.2
Complex 2, C4C5C6	125.0, 124.3, 124.8
M. jannaschii monoclinic form	
Complex C1C2C3	130.2, 129.6, 128.8
Complex C4C5C6	129.0, 130.3, 129.0
E. coli catalytic trimer	141.1, 135.8, 135.0
P. abyssi catalytic trimer + PALA	118.2
E. coli catalytic trimer + PALA	115.7, 116.1, 115.9
S. acidocaldarius T form	122.4
E. coli T form	123.1, 124.6
E. coli R form	115.1, 115.7

numbers of intermolecular contacts (complex 1, 229; complex 2, 138). The final map, contoured at 1.0σ, shows continuous density for most main-chain and side-chain atoms for both complexes with a few exceptions. Residues 74–82 and 126–129 have fragmented and/or weak density in all monomers. The C-terminus is well defined for chain C4 of complex 1 but poorly defined beyond residue 304 for most other chains. A few residues on the surface of the monomers do not have side-chain electron density. Complex 2 has weaker electron density overall than complex 1.

3.2. Description of the structure

The four crystallographically independent trimers in the asymmetric unit associate in pairs to form two complexes of trimers with 32 point-group symmetry, similar to the complex observed in the monoclinic form (Vitali *et al.*, 2008; Fig. 1). The two complexes are related by a rotation of 157.4° around the direction with spherical polar angles (ω, φ) = (82.4, −135.2°) and are similar to each other and to the complex in the monoclinic form. The superposition of the two complexes in the present structure is illustrated in Fig. 1(*b*). The r.m.s.d. between corresponding C^{α} atoms is 0.49 Å for the two complexes in the present structure and 1.32 and 1.16 Å for complexes 1 and 2, respectively, compared with the monoclinic complex. The monomers are similar, with an average r.m.s.d. between C^{α} atoms of all chains of 0.31 Å. The r.m.s.d. between corresponding C^{α} atoms of the central chains in the present structure and the monoclinic structure is 0.71 Å.

The planar angles (Table 2) are nearly constant in each trimer and are in the ranges 122.9–124.7° in complex 1 and 124.2–125.2° in complex 2. These values are up to 7.4° less than in the monoclinic form and are comparable to those in the *E. coli* T-form ATCase. Planar angles are sensitive indicators of domain movement and it is unlikely that they are affected by resolution (Stieglitz *et al.*, 2004; Vitali *et al.*, 2008). The variation in the planar angles between the crystal forms is large and may suggest high flexibility in solution and high reactivity even though the near-threefold symmetry in each trimer is maintained. The unliganded *E. coli* catalytic trimer shows variation of this angle within the same trimer and the threefold symmetry is not maintained (Beernink *et al.*, 1999).

The vertical association of the catalytic subunits in both complexes of the present structure is similar to that observed in the monoclinic

Table 3
Comparative analysis of the trimer–trimer interfaces of the *M. jannaschii* complexes in the present structure and the monoclinic form.

	Complex 1	Complex 2	Monoclinic form
Hydrogen bonds, ion pairs and hydrophobic contacts in C1–C4-type interfaces			
Hydrogen bonds	2–5	4	2
Salt bridges	0	0	0
% in networks	0	0	0
Hydrophobic	9–18	9–15	12–14
No. of hydrophobic pairs	8–12	7–9	8–10
ASA† buried, total	1014	1073	1048
ASA† buried, charged	266	244	226
ASA† buried, apolar	480	457	555
Hydrogen bonds, ion pairs and hydrophobic contacts in C1–C5-type interfaces			
Hydrogen bonds	1‡	1‡	1‡
Salt bridges	1–2§	1§	1§
% in networks	100	100	100
Hydrophobic	8–22	12–16	10–12
No. of apolar pairs	3–6	3–4	2
ASA†, buried total	610	572	811
ASA†, buried charged	247	209	414

† The ASA of the C1–C4-type interfaces was computed as the sum of the ASAs of all the monomers in the C complex minus the sum of the ASAs of the three C1–C4-type dimers divided by three. The same procedure was used for the C1–C5-type interfaces except that the C1–C5-type dimers were used in the calculation. ‡ Only in one interface. § In two of the interfaces.

form. Monomers of adjacent trimers have a staggered arrangement around the threefold axis in all three complexes, with torsional angles for C1–C4, C1–C6 and C1–C5 (Fig. 1) of −40.0, −159.8 and 79.9° (complex 1), −40.6, −160.5 and 79.6° (complex 2) and −44.4, −164.5 and 75.6° (monoclinic form). The inter-trimer distance in all three complexes is short at 33.8 Å. These torsional angles are sensitive indicators of the relative orientations of the catalytic subunits and are not likely to depend on resolution. The twist of −4.0° between the complexes of the orthorhombic and monoclinic forms demonstrates some flexibility in the relative rotation around the threefold axis at a constant inter-trimer distance. The interactions (Table 3) between the two trimers are across C1–C4-type and C1–C5-type interfaces and several are conserved among the *M. jannaschii* catalytic complexes. The differences in the relative rotations of the trimers between complexes correlate with small differences in the ASAs buried in these interfaces (Table 3). These parameters are known not to depend on resolution (Novotny *et al.*, 2007). The similarity between the association of the two catalytic trimers in the present structure and in the monoclinic form in different crystalline environments indicates that this arrangement is stable. However, size-exclusion chromatography studies have shown that the catalytic subunits exist as isolated trimers in Tris solution (Hack *et al.*, 2000). It is possible that the association we observe in the crystalline state occurs at high concentrations of the protein and/or in the presence of ammonium sulfate. Estimates of the hydrodynamic radius and molecular mass (58 Å and 205 000) from dynamic light-scattering measurements in 0.66 *M* ammonium sulfate are consistent with the formation of hexamers, as observed in the crystalline state, but these solutions show high polydispersity and the estimated values could be weighted averages of more than one species. Moreover, such molecular-weight estimates from dynamic light scattering involve assumptions about molecular shape that may not accurately represent the particles in solution. It is important to note that this novel association may also be part of the holoenzyme *in vivo* in the presence of the regulatory subunits.

Each trimer has a sulfate at the center of its three CP domains on the noncrystallographic threefold as was observed in the structure of the monoclinic form (Vitali *et al.*, 2008; Fig. 1*a*). Each sulfate is involved in an extended ion-pair network with all three monomers of its

trimer through charged residues of the α2 helix that point into the central channel. This network provides additional stability to the association of monomers to form a trimer. The sulfates most likely came from the crystallization medium.

3.3. Thermostability

Several structural features that could potentially contribute to the thermostability of the *M. jannaschii* catalytic trimer were identified in the monoclinic structure (Vitali *et al.*, 2008). These include (i) changes in the amino-acid composition such as a decrease in the thermolabile residues Gln and Asn, an increase in the charged residues Lys and Glu, an increase in Tyr residues and a decrease in Ala residues, (ii) shortening of the N-terminus and shortening of three loops and (iii) a larger number of salt bridges, in particular the improvement of ion-pair networks. The present structure confirms these conclusions. The possible association of the catalytic subunits with each other and with the regulatory subunits in the holoenzyme may provide additional thermostabilization *in vivo*.

4. Conclusions

Crystals of the catalytic subunit of *M. jannaschii* ATCase in an orthorhombic crystal form contain four crystallographically independent trimers in the asymmetric unit which are similar in structure to the catalytic trimers in the monoclinic form of the enzyme (Vitali *et al.*, 2008). Each trimer has a sulfate in the central channel. The catalytic subunits show large differences in their planar angles from the *C*2 form, indicating high flexibility and reactivity in solution. In both crystal forms the catalytic subunits associate in pairs to form similar staggered complexes of trimers with a short inter-trimer distance of 33.8 Å. This association shows flexibility in the rotation of the two trimers relative to each other around their common threefold axis. The formation of these complexes in three different crystalline environments in two different crystal forms indicates that they are stable. It is tempting to speculate that this association may be part of the holoenzyme *in vivo* in the presence of the regulatory subunits. The earlier study of the *C*2 form provided insight into some of the factors that potentially contribute to the thermostability of the trimer. The possible association of the catalytic subunits with each other, as observed in these complexes, and with the regulatory subunits in the holoenzyme may provide additional thermostabilization *in vivo*.

This work was supported in part by startup funds from Cleveland State University (JV) and grants GM071512 (JV) and GM008180 (MJC) from the National Institutes of Health. We thank Dr Evan Kantrowitz for providing the EK1911 strain that was used for this study, Dr Dieter Schneider of Brookhaven National Laboratory for use of his beamline X12B and for instruction and help during data collection and Dr Ewa Folta-Stogniew for the dynamic light-scattering measurements and discussions.

References

Allewell, N. M. (1989). *Annu. Rev. Biophys. Chem.* **18**, 71–92.
Beernink, P. T., Endrizzi, J. A., Alber, T. & Schachman, H. K. (1999). *Proc. Natl Acad. Sci. USA*, **96**, 5388–5393.
Brünger, A. T., Adams, P. D., Clore, G. M., DeLano, W. L., Gros, P., Grosse-Kunstleve, R. W., Jiang, J.-S., Kuszewski, J., Nilges, M., Pannu, N. S., Read, R. J., Rice, L. M., Simonson, T. & Warren, G. L. (1998). *Acta Cryst.* D**54**, 905–921.
De Vos, D., Van Petegem, F., Renaut, H., Legrain, C., Glansdorff, N. & Van Beeumen, J. J. (2004). *J. Mol. Biol.* **339**, 887–900.
Emsley, P. & Cowtan, K. (2004). *Acta Cryst.* D**60**, 2126–2132.
Endrizzi, J. A., Beernink, P. T., Alber, T. & Schachman, H. K. (2000). *Proc. Natl Acad. Sci. USA*, **97**, 5077–5082.
England, P., Leconte, C., Tauc, P. & Herve, G. (1994). *Eur. J. Biochem.* **222**, 775–780.
Hack, E. S., Vorobyova, T., Sakash, J. B., West, J. M., Macol, C. P., Herve, G., Williams, M. K. & Kantrowitz, E. R. (2000). *J. Biol. Chem.* **275**, 15820–15827.
Herve, G. (1989). *Allosteric Enzymes*, edited by G. Herve, pp. 61–79. Boca Raton: CRC Press.
Jin, L., Stec, B., Lipscomb, W. N. & Kantrowitz, E. R. (1999). *Proteins*, **37**, 729–742.
Jones, M. E., Spector, L. & Lipmann, F. (1955). *J. Am. Chem. Soc.* **77**, 819–820.
Jones, T. A., Zou, J.-Y., Cowan, S. W. & Kjeldgaard, M. (1991). *Acta Cryst.* A**47**, 110–119.
Kabsch, W. & Sander, C. (1983). *Biopolymers*, **22**, 2577–2637.
Ke, H. M., Lipscomb, W. N., Cho, Y. J. & Honzatko, R. B. (1988). *J. Mol. Biol.* **204**, 725–747.
Kim, R., Sandler, S. J., Goldman, S., Yokota, H., Clark, A. J. & Kim, S.-H. (1998). *Biotechnol. Lett.* **20**, 207–210.
Kissinger, C. R., Gehlhaar, D. K. & Fogel, D. B. (1999). *Acta Cryst.* D**55**, 484–491.
Kleywegt, G. J. (1996). *Acta Cryst.* D**52**, 842–857.
Laskowski, R. A., MacArthur, M. W., Moss, D. S. & Thornton, J. M. (1993). *J. Appl. Cryst.* **26**, 283–291.
Lipscomb, W. N. (1992). *Proceedings of the Robert A. Welch Foundation Conference on Chemical Research*, Vol. XIII, pp. 103–143. Houston: Robert A. Welch Foundation.
Lipscomb, W. N. (1994). *Adv. Enzymol.* **68**, 67–152.
McDonald, I. & Thornton, J. (1994). *J. Mol. Biol.* **238**, 777–793.
Matthews, B. W. (1968). *J. Mol. Biol.* **33**, 491–497.
Novotny, M., Seibert, M. & Kleywegt, G. J. (2007). *Acta Cryst.* D**63**, 270–274.
Otwinowski, Z. & Minor, W. (1997). *Methods Enzymol.* **276**, 307–326.
Stevens, R. C., Gouaux, J. E. & Lipscomb, W. N. (1990*a*). *Biochemistry*, **29**, 7691–7701.
Stevens, R. C., Gouaux, J. E. & Lipscomb, W. N. (1990*b*). *Biochemistry*, **29**, 11146.
Stieglitz, K., Stec, B., Baker, D. P. & Kantrowitz, E. R. (2004). *J. Mol. Biol.* **341**, 853–868.
Van Boxstael, S., Cunin, R., Khan, S. & Maes, D. (2003). *J. Mol. Biol.* **326**, 203–216.
Vitali, J., Colaneri, M. J. & Kantrowitz, E. R. (2008). *Proteins*, **71**, 1324–1334.
Williams, M. K., Stec, B. & Kantrowitz, E. R. (1998). *J. Mol. Biol.* **281**, 121–134.